Journal of Science and Technology in Civil Engineering, HUCE, 2023, 17 (4): 66–79

SIMPLIFIED APPROACH FOR QUANTITATIVE ANALYSIS OF HARDENED CONCRETE MICROSTRUCTURE USING AUTOCORRELATION FUNCTION

Vu Chi Cong[a,*]

[a]*Faculty of Building and Industrial Construction, Hanoi University of Civil Engineering, 55 Giai Phong road, Hai Ba Trung district, Hanoi, Vietnam*

Article history:
Received 25/4/2023, Revised 03/8/2023, Accepted 10/8/2023

Abstract

In this paper, the internal microstructures of three different concrete mixtures were investigated through digital image analysis procedure conducted on a set of 60 cross-sectional images of hardened concrete specimens. To quantitatively describe the geometry and spatial organization of all the components within the hardened concretes and measure the heterogeneity of different concrete mixtures and sample shapes, a two-dimensional Autocorrelation Function (ACF) analysis program was performed on a series of 60 scanned images of internal cross-sectional images. This enabled us to define a correlation range called the microstructural characteristic length, l_i, which can be used as: (i) an indicator to quantify the properties on the domain size of the internal microstructure of hardened concrete, and (ii) an input parameter for constitutive modeling or for estimating the Representative Volume Element (RVE) of concrete. As the image analysis procedure based on ACF does not require the segmentation of the images, the method proposed in the present paper provides a simple and useful way of quantifying the microstructure of concrete for many practical purposes.

Keywords: concrete; autocorrelation function; integral range; image analysis; characteristic length scale; microstructural characterization.

https://doi.org/10.31814/stce.huce2023-17(4)-06

1. Introduction

Concrete is a complex heterogeneous material with hardened structures consisting of a variety of different components, i.e. aggregates, multi-scale pores, air voids, and cement matrix. The internal structure of hardened concrete is hence affected by multiple factors, such as the size and shape of the aggregates, the cement paste, the interfacial transition zone (ITZ) between the cement paste and aggregates, the spatial distribution of the components, and the degree of compaction [1]. It is widely acknowledged that the internal structure of concrete has a significant impact on its mechanical responses of concrete under various loading conditions [2]. Therefore, quantifying the microstructural characteristics of hardened concrete is frequently required in both numerical and experimental investigations of its mechanical behavior [3, 4]. For this purpose, several characteristic length scales have been proposed to describe the internal structures of concrete on the domain size. Those can be, for instance, the largest or the average size of aggregates, the size of pores, the ITZ length, etc., which can be applied for different types of concrete [5]. However, these defined characteristic lengths are not objective and precise as they do not provide a quantitative description of the spatial distribution, geometries, and fraction content of the various components that exist within the hardened concrete samples.

*Corresponding author. *E-mail address:* congvc@huce.edu.vn (Cong, V. C.)

In general, statistical correlation functions are frequently employed as a crucial technique in quantitatively characterizing the internal structures of heterogeneous materials such as concrete [6–9]. Anisotropic characteristics, orientation distribution, shape, and geometrical features can be extracted from the application of *n*-point correlation functions [6, 7, 9, 10] or Autocorrelation functions [11, 12] on the two-dimensional cross-sectional images of materials. The *n*-point spatial correlation function is a statistical method used to assess the likelihood of finding n points, in a predetermined geometrical arrangement, all located within the region of space occupied by a single constituent of a two-phase material [4, 10]. This means that, to apply *n*-point correlation functions, the heterogeneities existing in the internal structure of heterogeneous materials must be categorized into two distinct phases. In other words, the use of *n*-point correlation functions requires the segmentation of the individual components of the material. Nevertheless, this work is challenging and time-consuming due to the need for complex mathematical algorithms for image segmentation. On the other hand, the Autocorrelation Function (ACF) provides a simpler alternative that does not involve segmenting the individual components of the material. This approach avoids the potential biases that may arise from identifying component boundaries, and is therefore more practical. The ACF is capable of detecting the size, shape, orientation, and spatial arrangement of objects within an image [13]. Hence, it can serve as an effective tool to (i) provide a quantitative characterization of the internal structure of the material in a general sense, and (ii) objectively identify a Representative Volume Element (RVE) of the material in terms of microstructural properties [14]. ACF is widely used in the field of geology and geosciences due to its ability to analyze visual textures (color objects), as opposed to the binary objects that the *n*-point correlation functions consider [11, 12]. Conversely, the application of ACF for concrete has not been extensively studied thus far.

This paper presents an image analysis procedure conducted on cross-sectional images of various hardened concrete specimens to investigate their microstructural features. Subsequently, an ACF analysis program was implemented on a set of 60 scanned images of the cross-sections of the specimens to analyze the internal microstructure of the three examined concretes. This allowed for the identification of a characteristic length of the microstructure, denoted as l_i, which can be used to quantitatively describe the internal microstructure of the hardened concrete in its entirety.

2. Theoretical background

2.1. Principles of Autocorrelation Function

In the context of image analysis, the Autocorrelation Function (ACF) provides information about the degree of correlation between an image and a displaced version of itself. More specifically, it measures the extent to which the gray values of individual pixels are correlated with those of neighboring pixels as a function of their relative spatial displacement [13, 15]. To determine the ACF of a digital image, a duplicate of the original image is shifted by different displacements in all directions and the autocovariance is computed as a function of the displacement [12, 13, 15]. For an image of size M×N pixels, ACF can be calculated by Eq. (1).

$$C(a,b) = \sum_{x}^{M} \sum_{y}^{N} i(x,y) * i(x+a, y+b) \tag{1}$$

where $C(a,b)$ is the autocorrelation function, $i(x,y)$ is the two-dimensional grey value at position (x,y), and a and b represent the displacement (or lag) from the corresponding x and y positions. Similar to the original image, the ACF is also a two-dimensional function. Despite having the same dimensions, the ACF and the original image have different significance. In the original image, a

coordinate point (x, y) represents a position, whereas in the ACF, a coordinate point $(a,\ b)$ refers the endpoint of a neighborhood vector. Moreover, the value of the ACF at a given point (a, b) indicates the correlation of all image points (x, y) with all neighbourhood points located at $(x + a, y + b)$. In the context of digital images, the application of ACF can offer insights into the primary features or spatial attributes present within the images. These may include characteristics such as the directionality or periodicity of specific patterns.

The ACF is commonly associated with Fourier analysis and the implementation of Fast Fourier Transforms (FFT) [13]. While both methods are mathematically equivalent to Eq. (1), the FFT method provides greater computational efficiency [16, 17]. On the image plane, a Region of Interest (ROI) which must be square to allow the use of FFT algorithms, is selected and digitized [12, 13, 15]. Following the works of Heilbronner et al. [11, 13], the ACF of an image is typically computed using the following procedure:

(i) The digitized ROI of a given image is read into a matrix of gray values. Note that ROI must be square.

(ii) The mean gray value $\overline{i\,(x, y)}$ is calculated and subtracted as follows:

$$f(x, y) = i(x, y) - \overline{i(x, y)} \tag{2}$$

(iii) The two-dimensional discrete Fourier transform is given by:

$$f(u, v) = \frac{1}{N} \sum_{x=0}^{N-1} \sum_{y=0}^{N-1} f(x, y).\exp\left[-2\pi i(ux + vy)/N\right] \tag{3}$$

where $f\,(u, v)$ is the discrete transform, u and v are the frequencies in $x-$ and $y-$ direction, $f\,(x, y)$ is the discrete gray value at the position (x, y), x and y are the discrete image coordinates, $N = 2^m$ (where m is an integer) is the size of the matrix (or the size of digitized ROI of an image), and i is $\sqrt{-1}$.

(iv) The transform is calculated via the application of the separability theorem using the following expression:

$$f(u, v) = \frac{1}{N} \sum_{x=0}^{N-1} f(x, v).\exp\left[-2\pi i(ux)/N\right] \tag{4}$$

where

$$f(x, v) = \frac{1}{N} \sum_{y=0}^{N-1} f(x, y).\exp\left[-2\pi i(vy)/N\right] \tag{5}$$

Eqs. (4) and (5) indicate that the rows and columns of the image matrix are transformed using two sequential one-dimensional FFTs.

(v) The Fourier transform of the ACF is acquired by multiplying the Fourier transform of the image, $f\,(u, v)$, with its complex conjugate $f^*\,(u, v)$.

(vi) Next, the inverse transformation is applied to calculate the value of ACF, $g\,(x, y)$ at the position (x, y) as follows:

$$g(x, y) = \frac{1}{N} \sum_{u=0}^{N-1} \sum_{v=0}^{N-1} f(u, v).\exp\left[-2\pi i(ux + vy)/N\right] \tag{6}$$

In this study, the Autocorrelation function value at the point (x, y), $C\,(x, y)$, is finally calculated by normalizing the value $g\,(x, y)$ obtained from Eq. (6) with its maximum value (i.e. $g\,(0, 0)$).

2.2. *Definition of microstructural characteristic length*

As mentioned in Section 1, the ACF of a digital image can provide global information for all features contained in an image with regard to geometry. Those are, for instance, the average shape, the preferred orientation, the isotropy or anisotropy behavior, and the spatial organization of the microstructural features (e.g. grains, pores, cement paste, etc.) [12, 15]. However, the two-dimensional ACF itself cannot express the microstructural characteristics in terms of size. For this work, a range which gives information on the domain size of the microstructural characteristics has to be extracted from the ACF. This range is commonly called Autocorrelation length (ACL). Several methods have been proposed based on the definition that autocorrelation length measures the rate at which a random event decays [7, 18, 19]. For instance, some researchers [18–20] employed exponential functions to describe the ACF and determined the ACL as the displacement at which the ACF decreases to $1/e$ of its original value. Alternatively, some authors [6, 7] estimated the ACL as the distance at which the ACF reaches a constant value (e.g. the square of the volume fraction of examined object or zero). This distance (or ACL value, r_0) implies that the correlation between $f(x, y)$. and $f(x + r_0, y + r_0)$ is considered to be vanished. Consequently, the ACL can be applied for estimating the dimensions of the Representative Volume Element (RVE) of the material [3, 21]. The value of the ACL is frequently observed to be proportional to the size of the largest relevant features (or heterogeneities) within a given microstructure [6, 13, 22]. Consequently, r_0 is insufficient to quantify the spatial properties such as the shape, orientation, volume fraction of the heterogeneities presented in the image.

Another definition for a range that can be used to quantitatively describe the microstructure is called the integral range [14, 23, 24]. The definition of the integral range in the space R^n is:

$$l_i = \frac{1}{C(x,0) - C(x,r_0)} \int_{R^n} (C(x,r) - C(x,r_0)dr \tag{7}$$

where $C(x,0)$ is the value of the ACF at zero displacement ($r = 0$), and r_0 is the autocorrelation length. According to [3, 14], this integral range is significant parameter to predict the variability of material properties as a function of the geometry of parts. In other words, it can be used the integral range, l_i, to globally characterize the microstructure of a material. Based on this, in the present study, we define the microstructural characteristic length as the integral range that is calculated from an integration of the ACF following Eq. (7).

An example of the relationship between the ACF value, $C(x,r)$, and the displacement, r, for a given direction is shown in Fig. 1. The highest ACF value is equal to 1, which corresponds to zero displacement ($r = 0$). As the displacement r increases, the ACF value gradually decreases until it reaches zero. As seen in Fig. 1, the points with a displacement larger than r_0 are uncorrelated ($C(x, r > r_0) \sim 0$). Therefore, r_0 can be considered as the autocorrelation length of the microstructure. In this study, r_0 is defined as the distance from the origin to the point where ACF reaches a value of 0 for the first time (see Fig. 1). From Eq. (7), for a given direction (x = const), the defined microstructural characteristic length, l_i, can be now estimated by the following equation:

$$l_i = \int_0^{r_0} (C(r) - C(r_0))dr \tag{8}$$

In this study, both the ACL value, r_0, and the integral range, l_i, are considered in quantitatively characterizing the microstructure of hardened concrete samples.

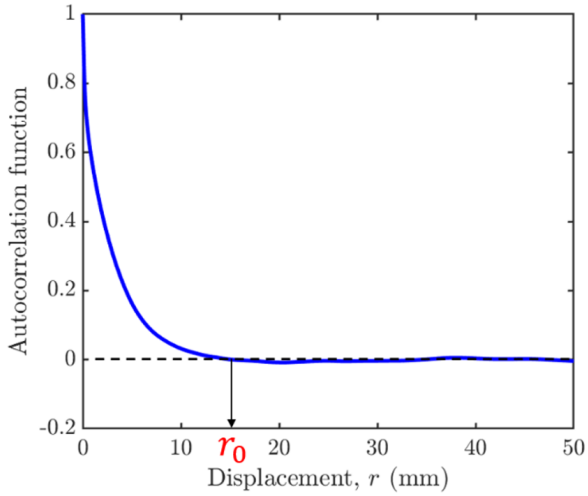

Figure 1. An example of the relationship between the ACF value, $ACF\,(x, r)$, and the displacement, r, for a given direction

3. Materials and Image analysis

3.1. Materials and samples preparation

In the present work, three mixtures of normal-weight concrete were examined. Mix proportions for these three concretes are presented in Table 1. Ordinary Portland cement with the properties satisfying the specifications outlined in [25] was used for all mixtures. Concrete was cast using portable tap water. The sand and coarse aggregates employed in all the mixtures complied with the requirements described in [26]. The size distribution of the aggregates, determined via sieve analysis, was consistent with [27]. In this study, the maximum size of aggregate, d_a, was defined as the nominal sieve aperture size for which the mass of the retained fraction was below 10%.

For a specific concrete mix proportion, both 150×300 mm concrete cylinders and 150 mm concrete cubes were considered. The casting and curing procedures of concrete specimens were performed in accordance with the protocol for normal-weight concrete outlined in [28].

Table 1. Mix proportions of 1 m^3 concrete mixtures

Concrete mixture	Cement:sand:coarse aggregate (by weight)	Water-to-Cement ratio	The maximum size of aggregates, d_a (mm)
M1	1:3:0	0.5	2.5
M2	1:2.2:2.7	0.43	10
M3			20

Two samples of each mixture and each shape, for a total of 12 concrete specimens, were used for the image analysis works in this study. These specimens were cut by using diamond grinding discs at 28 days of age. The cylindrical specimens were cut into four parts (Fig. 2(a)), while the cubes were cut into three pieces (Fig. 2(b)), for a total of 60 cross sections of concrete samples were prepared for the image analysis program in this study. To achieve high-quality images, the cross-section surfaces were first ground flat using hand pressure on a water-cooled wheel topped with more and more grit size of metal-bonded diamond plates, and then polished using successively finer grit resin-bonded diamond plates. After polishing, the surfaces were thoroughly cleaned with water. The polish was considered

acceptable if the surface had uniform reflectivity and was free of striations caused by the grinding materials.

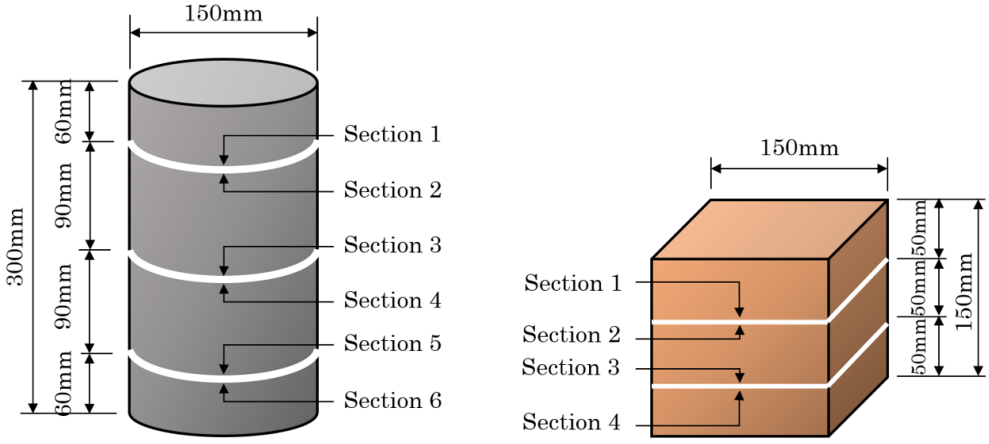

(a) Cylindrical samples (b) Concrete cubes

Figure 2. Cutting positions of the cross sections

3.2. Image analysis via Autocorrelation function

Two-dimensional color images of the concrete sample sections were acquired using a flatbed scanner. This scanner was set to a resolution of 1200 dpi to obtain the 24-bit color (RGB) digital image of the cross-section surfaces (Fig. 3).

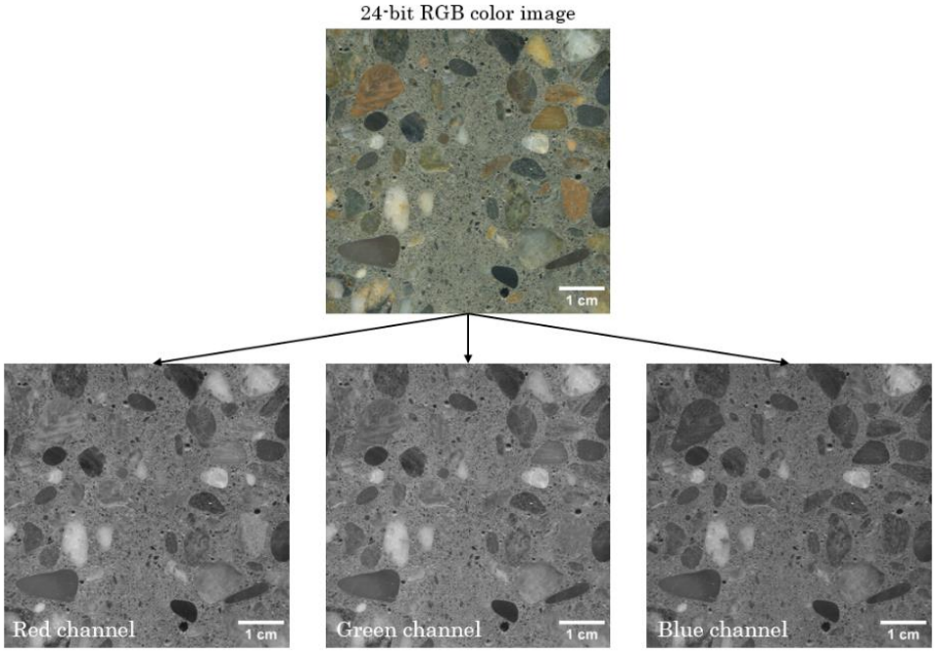

Figure 3. Three 8-bit gray scale images (Red, Green, and Blue channels) of a 24-bit color image

In the context of digital image analysis, an RGB color image can be considered as a stack of three channels, representing the Red, Green, and Blue intensity values for each pixel. This means that a 24-bit color value of each pixel is represented by a triplet of grayscale values, specifying the

relative magnitude of red, green, and blue components (see Fig. 3). In this study, for ACF analysis, the original RGB color image was split into three 8-bit grayscale images through the MATLAB^{TM} function of *rgb2gray*. In an 8-bit grayscale image, each pixel contains the color intensity information in a range from 0 (black color: darkest part) to 255 (white color: brightest part).

To determine the ACF values of an RGB image, the average of its three-color channels was computed. It is noteworthy that, for the ACF computation using the Fast Fourier Transform (FFT) algorithms, the image needs to be transformed into a square matrix. Consequently, 90 square regions of interest (ROIs) for circular sections (i.e. from the cylindrical specimens) which rotated around the center of the circular image were analyzed. The ACFs of these ROIs were calculated and then averaged. In this study, the Autocorrelation length, r_0, and the defined microstructural characteristics length, l_i, along a given direction of ACF are determined following the procedure described in Section 2. The values of r_0 and l_i of each grayscale image are calculated by averaging all the corresponding values obtained from all directions of its image plane, while those of each color cross-section image are averaged over its three-color channels.

4. Results and discussions

4.1. Features of autocorrelation function

Fig. 4 shows the ACF values of the examined sections for three concrete mixtures. Brighter regions on the ACF image represent a greater degree of spatial correlation, which are commonly called the "central peak" area of ACF [13, 15]. This central peak area is typically larger when the objects presented within the image (i.e., aggregates) are larger. Indeed, as shown in Fig. 4, the central peak area of the ACF for M1 mixture (Fig. 4(a)) was significantly smaller in comparison to those for M2 mixture (Fig. 4(b)) and M3 mixture (4(c)).

The ACF image consistently exhibits a single maximum value at its center, regardless of the concrete mixture or cross-section surface. From this peak value, the ACF gradually decreases to zero as the shifted displacement of the image (r) is increased. Nevertheless, owing to the anisotropic shape of the objects in the image, the rate of decrease of the ACF value away from the origin is not the same in all displacement directions. The rate of decay of the ACF away from the origin for the three concrete mixtures considered in this study can be ordered as follows: M1 < M2 < M3. This implies that M1 mixture contains fewer anisotropic objects than M2 and M3 mixtures do. In other words, the finer material (M1 mixture) exhibits better homogeneity compared to the coarser materials (M2 and M3 mixtures). This phenomenon can also be viewed from the "background" areas of the ACF image which correspond to the darker zone surrounding the central peak area. In the background area, the degree of fluctuation around zero for M1 concrete is significantly lower compared to that of M2 and M3 concretes (see Fig. 4).

The relationship between the ACF values, $C(x, y)$, and the displacement, r, for different sections, sample shapes, and mixtures are displayed in Fig. 5 and Fig. 6, from which it can be found that:

(i) for a given concrete sample, the ACFs of the different cutting sections of M1 and M2 mixtures are not significantly different, regardless of the concrete mixture and sample shape (Fig. 5). This implies that there is no segregation of the internal microstructures of hardened samples for these two mixtures. A quite difference is observed for the different sections of M3 mixture (Fig. 5(e) and (f)). This may result from the different sizes and content of the coarse aggregates presented within the sections of M3 mixtures. However, this difference is a qualitative observation and is not large enough to conclude that a segregation phenomenon exists within the M3-mixture samples.

(ii) for a given shape of the sample, the difference of the ACFs between the different sections in the same concrete sample is more pronounced with an increase in aggregate size. This agrees

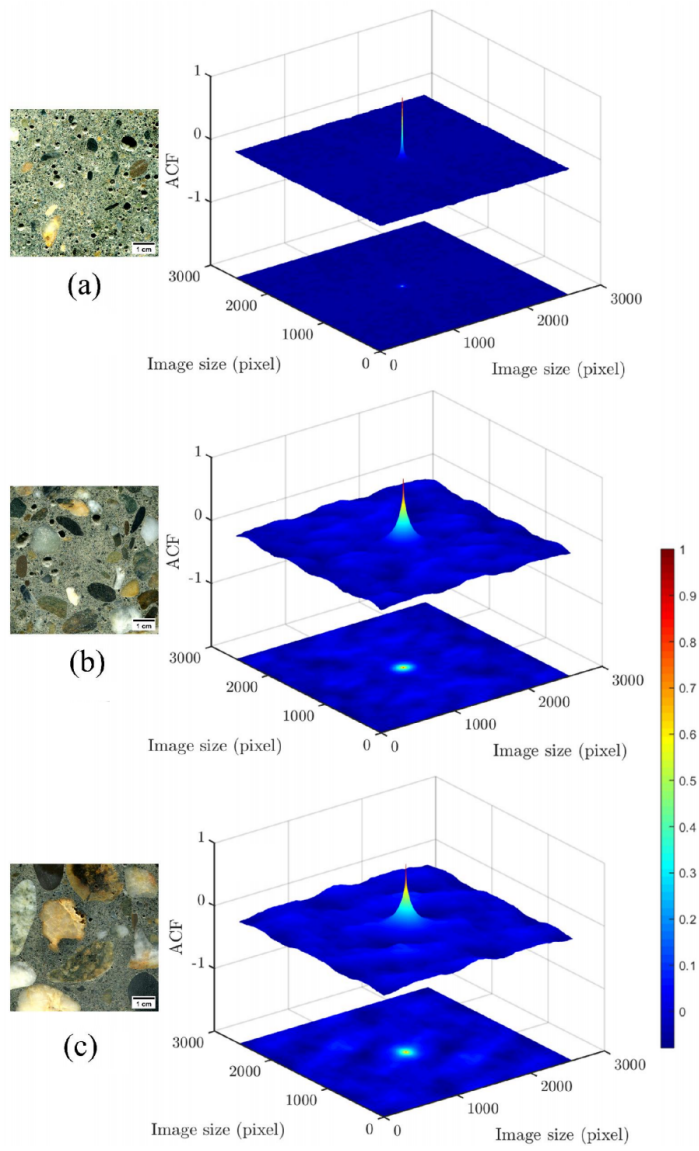

Figure 4. ACF for three concrete mixtures: (left) original scanned images; (right) digital image of ACF for (a) M1-, (b) M2-, and (c) M3-concrete mixtures

with the heterogeneous phenomenon observed from the ACF images above (Fig. 4). Indeed, when the aggregate sizes increase, the heterogeneity of the microstructure consequently increases, which causes more importance for the anisotropic behavior of the original image and the ACF image as well. As a result, the decay of the ACF away from the center is not the same in all directions and all sections.

(iii) On average, there is no significant difference in the relationship between ACF values ($C(x, y)$) and the displacement (r) among all sections of the cylinder and the cube of M1 and M2 mixtures (Fig. 6(a) and (b)), while a distinct difference is observed for M3 mixture (Fig. 6(c)). This finding implies that the shape and/or the size of the sample can affect the variation in hardened microstructure of a given concrete mixture.

(iv) as expected, a noticeable correlation exists between the ACF value and the size of the aggre-

gates (Fig. 6(d)). This indicates that the microstructural characteristics of the hardened concrete are mainly controlled by the size of the aggregates, without being influenced by the mix proportion.

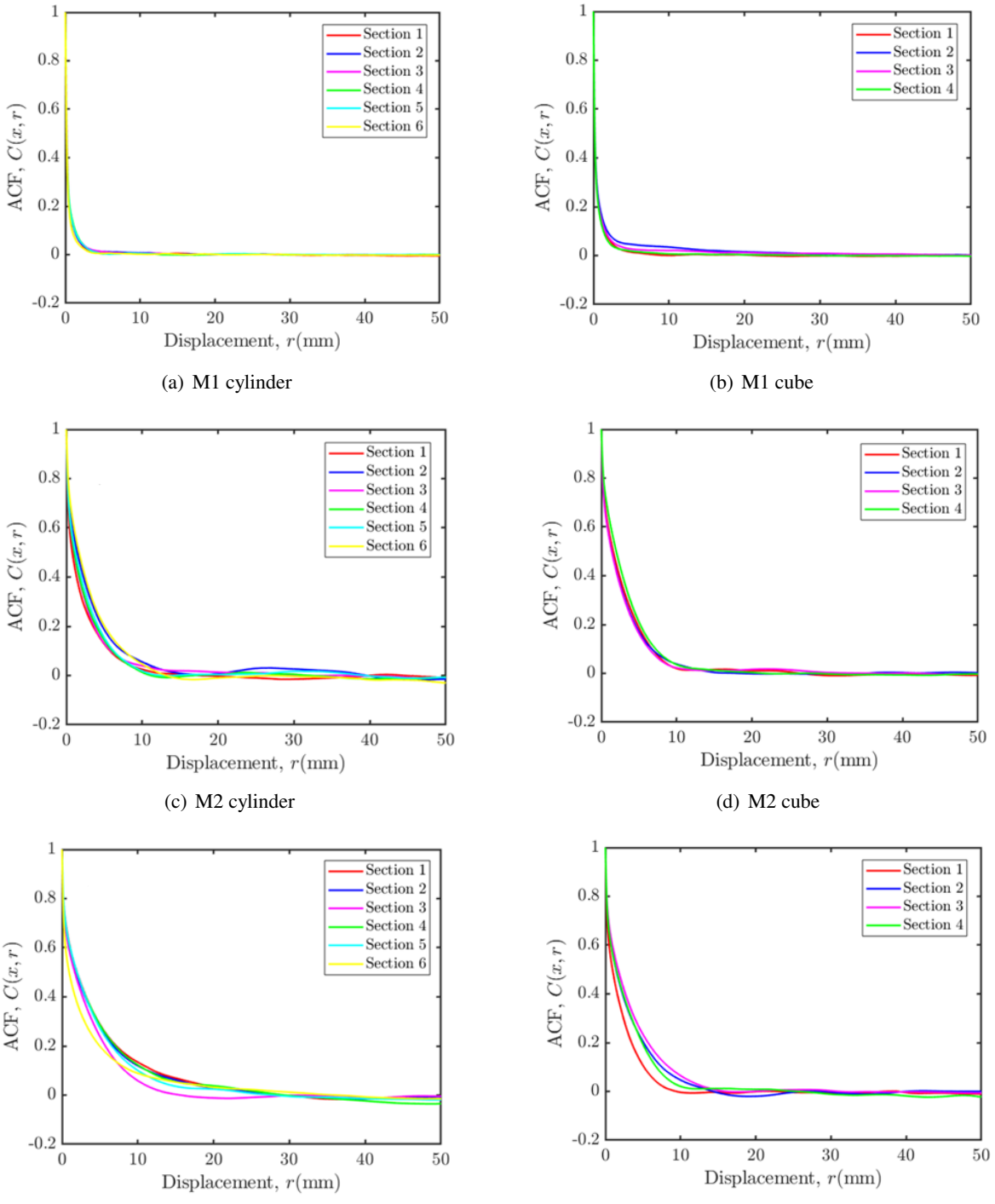

(a) M1 cylinder

(b) M1 cube

(c) M2 cylinder

(d) M2 cube

(e) M3 cylinder

(f) M3 cube

Figure 5. The relationship between ACF value, $C(x, r)$, and the displacement, r, for different sections

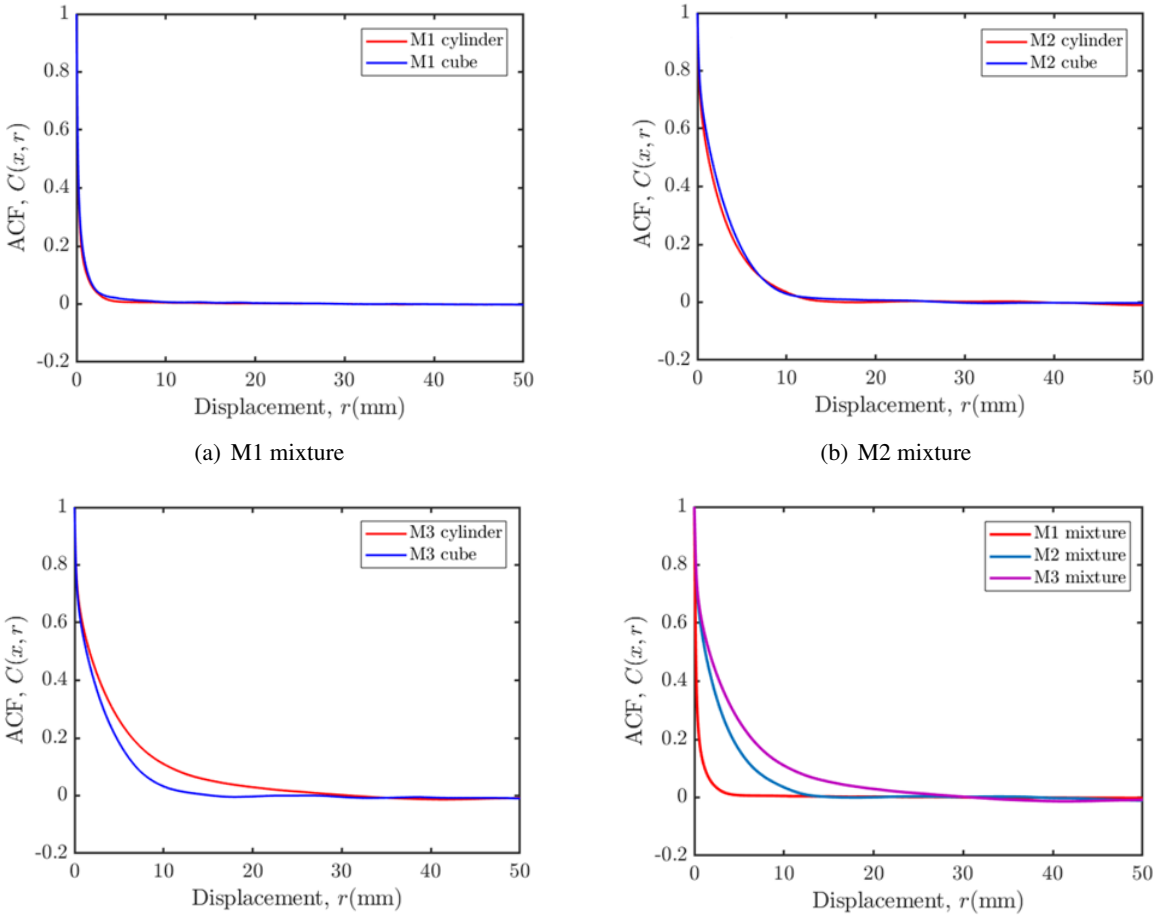

(a) M1 mixture

(b) M2 mixture

(c) M3 mixture

(d) All cutting sections of the three examined concrete mixtures

Figure 6. The relationship between ACF value, $C(x,r)$, and the displacement, r, for different shapes

4.2. Autocorrelation length

As previously mentioned in Subsection 2.2, this study defines the autocorrelation length, r_0, as the displacement where the ACF remains positive (see Fig. 1). The values of r_0 for different samples and concrete mixtures are summarized in Table 2 and Fig. 7, from which, it is observed that:

(i) for a specific concrete mix proportion, the values of autocorrelation length (ACL), r_0, of cylinders and cube are similar. This demonstrates that the ACL value is not influenced by the shape of the concrete sample. Additionally,

(ii) for a given shape of the concrete sample, both the mean value and the standard deviation (SD) of r_0 increase as the size of aggregates, d_a, increases, meaning that the ACL value is strongly affected by the size of the aggregates. This is clearly seen from a linear correlation between r_0 and d_a ($r_0 \sim 1.5d_a$) presented in Fig. 8. This finding suggests that to achieve comparable hardened microstructures among different concrete samples for the three mixtures examined in this study, the characteristic dimension of the samples should be greater than 1.5 times the maximum aggregate size.

Table 2. Autocorrelation length, r_0, and microstructural characteristic length, l_i, averaged over all sections for the three examined concrete mixtures

Concrete specimen	r_0 (mm)		l_i (mm)		Concrete group	r_0 (mm)		l_i (mm)	
	Mean	SD	Mean	SD		Mean	SD	Mean	SD
M1 cylinder	6.5	2.7	0.66	0.11	M1 mixture	6.9	4.3	0.67	0.16
M1 cube	7.3	3.4	0.67	0.12					
M2 cylinder	18.3	5.4	2.21	0.28	M2 mixture	18.8	8.2	2.32	0.34
M2 cube	19.2	6.2	2.43	0.20					
M3 cylinder	29.0	7.1	3.74	0.69	M3 mixture	28.1	12.5	3.62	0.92
M3 cube	27.2	13	3.49	0.60					

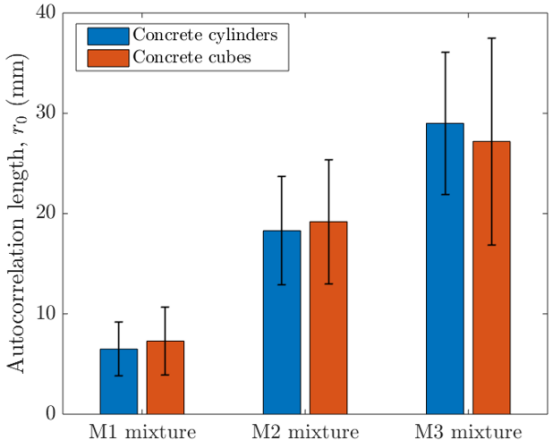

Figure 7. Autocorrelation length, r_0, for different specimens of the three examined concrete mixtures

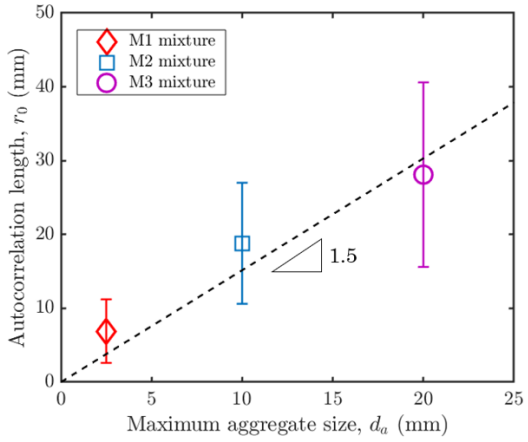

Figure 8. Relationship between the value of Autocorrelation length, r_0, and the maximum size of aggregates, d_a

4.3. Microstructural characteristic length

The variations of the defined microstructural characteristic length, l_i, regarding different samples of the three concrete mixtures considered in this study are shown in Fig. 10. Similar to the ones presented in Fig. 7, it is observed that there is no significant influence of sample shape on the value of l_i, irrespective of concrete mix proportion. This suggests that the microstructural characteristic length, l_i, as defined in this study, can serve as a useful metric for measuring the discrepancy in microstructural properties among various samples of a given material. Furthermore, for whatever the shape of the concrete sample, when the maximum size of the aggregates increases, the defined characteristic length of hardened microstructure, l_i increases in terms of both the mean value and variability (see Fig. 9 and Table 2). This finding indicates that the heterogeneity of hardened concrete increases with an increase in aggregate size, which is consistent with the qualified observations presented in Subsection 4.3 regarding the values of ACF.

On average, the defined microstructural characteristic length, l_i, exhibits a linear correlation with the maximum size of the aggregates, d_a, with a proportionality coefficient of 0.2 ($l_i \sim 0.2d_a$) (see Fig. 10). This relationship allows us to conclude that (i) the microstructure of the hardened concrete is mostly affected by the aggregates, and (ii) l_i can also be used to represent the structure of aggregates

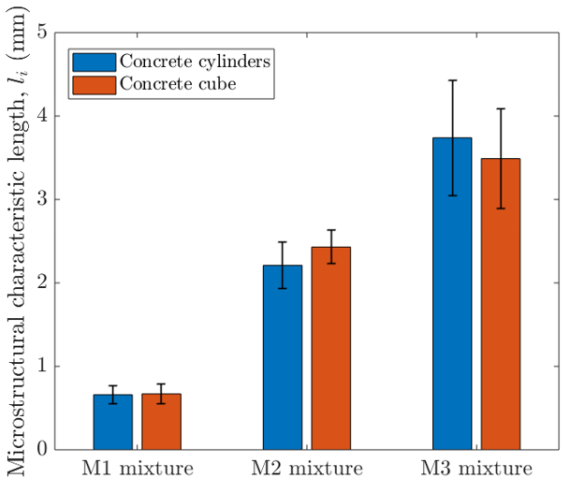

Figure 9. Values of the defined microstructural characteristic length, l_i, for different samples of the three examined concrete mixtures

within hardened concrete sample. The strong influence of aggregate size on both the autocorrelation length, r_0, and the characteristic length, l_i, arises from the fact that, for the conventional normal-weight concrete like the three examined in this study, the aggregates possess the highest volume fraction among the components of hardened concrete samples, including pores, air voids, and cement matrix. As a result, the ACF values are mainly controlled by the aggregates which represent the primary and most voluminous objects presented in cross-section images of concrete (see Fig. 3 and Fig. 4).

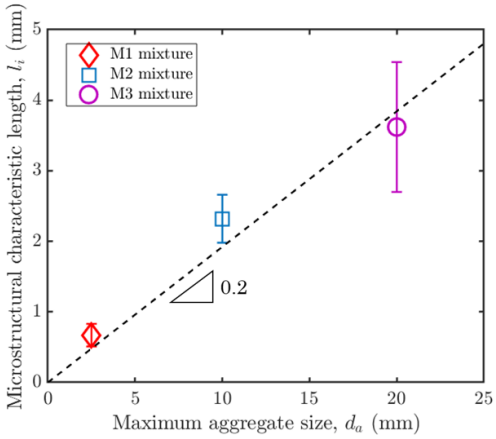

Figure 10. Relationship between the value of microstructural characteristic length, l_i, and the maximum size of aggregates, d_a

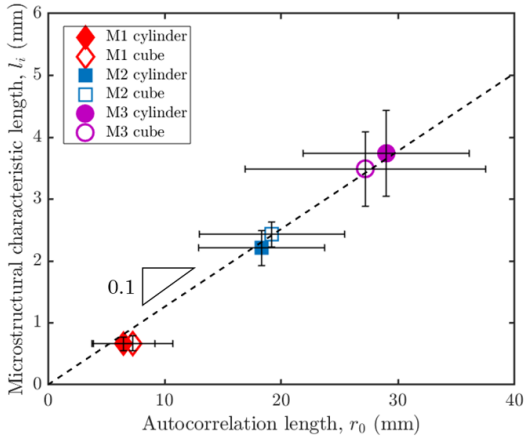

Figure 11. Relationship between the value of microstructural characteristic length, l_i, and the autocorrelation length, r_0

As shown in Fig. 11, there is a clear correlation between the autocorrelation length, r_0, and the defined microstructural characteristic length, l_i, regardless of sample shape and concrete mix proportion. The value of l_i is observed to be about one order of magnitude smaller than the value of r_0. Moreover, the associated variabilities of the characteristic length, l_i, are always significantly lower than those of the autocorrelation length, r_0, (see Fig. 11 and Table 2), meaning that l_i is more reliable measure than r_0 in terms of providing consistent values for microstructural quantification.

Alternatively, as an integral range (see Subsection 2.2), the characteristic length, l_i, can provide a

quantitative representation of the shape of the ACF. In other words, l_i can serve as a quantitative descriptor of the microstructural features of a hardened concrete sample in its entirety. Meanwhile, the autocorrelation length, r_0, can solely portray the magnitude of the principal objects (i.e. aggregates in this study) exhibited in the image [13]. To summarize, the defined microstructural characteristic length, l_i, should be used to quantify the internal structure of hardened concrete rather than the autocorrelation length, r_0. This also suggests that the characteristic length, l_i, can serve as a suitable measure of the representative volume element (RVE) size for concrete.

5. Conclusions

In the present work, the microstructural characteristics of hardened concrete samples prepared from the three different mixtures were qualitatively and quantitatively investigated through the image analysis procedure performed on scanned image of cross-sections of concrete. The definition of the microstructural characteristic length, l_i, which is derived from the two-dimensional autocorrelation function, serve as a useful and straightforward tool for measuring the internal structure of hardened concrete. From the variations of this characteristic length, it concludes that for conventional normal-weight concrete, the hardened structure is mostly controlled by the aggregates. Additionally, the defined characteristic length, l_i, can be used as a parameter to quantify the heterogeneity of a heterogeneous material such as concrete.

The image analysis procedure and the microstructural characteristic length proposed in this study can be applied for other purposes, for instance, quantifying the segregation phenomenon in concrete or comparing concrete samples with a given mix proportion supplied from different sources. In addition, the defined characteristic length could be beneficial for modeling concrete, as it serves as a suitable quantifying dimension for the internal microstructure that can be integrated into constitutive relations.

The present research focuses solely on exploring the internal structure of hardened conventional normal-weight concrete. However, the methods employed in this study can be applied to examine other types of concrete, such as fiber concretes, self-compacting concrete, and ultra-high performance concrete, where the aggregates (especially coarse aggregates) are not the primary component and their sizes might not have a significant effect on the hardened microstructure.

References

[1] Brooks, A. M., Neville, J. J. (2010). *Properties of concrete*. 4th edition, Pearson Education Limited.

[2] Masad, E., Muhunthan, B., Shashidhar, N., Harman, T. (1999). Internal structure characterization of asphalt concrete using image analysis. *Journal of Computing in Civil Engineering*, 13(2):88–95.

[3] Jeulin, D., Ostoja-Starzewski, M. (2001). *Mechanics of random and multiscale microstructures*. Springer Vienna.

[4] Torquato, S. (1991). Random heterogeneous media: microstructure and improved bounds on effective properties. *Applied Mechanics Reviews*, 44(2):37–76.

[5] Bazant, Z. P., Planas, J. (1998). *Fracture and size effect in concrete and other quasibrittle materials*. CRC Press, Boca Raton, Florida, USA.

[6] Falchetto, A., Moon, K., Wistuba, M. (2014). Microstructural analysis and rheological modeling of asphalt mixtures containing recycled asphalt materials. *Materials*, 7(9):6254–6280.

[7] Moon, K. H., Falchetto, A. C., Jeong, J. H. (2014). Microstructural analysis of asphalt mixtures using digital image processing techniques. *Canadian Journal of Civil Engineering*, 41(1):74–86.

[8] Velasquez, R. A. (2009). *On the representative volume element of asphalt concrete with applications to low temperature*. University of Minnesota.

[9] Jiao, Y., Stillinger, F. H., Torquato, S. (2008). Modeling heterogeneous materials via two-point correlation functions. II. Algorithmic details and applications. *Physical Review E*, 77(3):031135.

[10] Baniassadi, M., Ahzi, S., Garmestani, H., Ruch, D., Remond, Y. (2012). New approximate solution for N-point correlation functions for heterogeneous materials. *Journal of the Mechanics and Physics of Solids*, 60(1):104–119.
[11] Heilbronner, R. (2002). Analysis of bulk fabrics and microstructure variations using tesselations of auto-correlation functions. *Computers & Geosciences*, 28(4):447–455.
[12] Pfleiderer, S., Ball, D. G. A., Bailey, R. C. (1993). AUTO: A computer program for the determination of the two-dimensional autocorrelation function of digital images. *Computers & Geosciences*, 19(6): 825–829.
[13] Heilbronner, R., Barrett, S. (2014). *Image analysis in earth sciences: Microstructures and textures of earth materials*. Springer Berlin Heidelberg.
[14] Kanit, T., Forest, S., Galliet, I., Mounoury, V., Jeulin, D. (2003). Determination of the size of the representative volume element for random composites: statistical and numerical approach. *International Journal of Solids and Structures*, 40(13–14):3647–3679.
[15] Heilbronner, R. P. (1992). The autocorrelation function: an image processing tool for fabric analysis. *Tectonophysics*, 212(3–4):351–370.
[16] Gonzalez, R. C., Woods, R. E. (2002). *Digital image processing*. 2nd edition, Prentice Hall Press.
[17] Jähne, B. (2005). *Digital image processing*. 6th edition, Springer Science & Business Media.
[18] Berryman, J. G. (1985). Measurement of spatial correlation functions using image processing techniques. *Journal of Applied Physics*, 57(7):2374–2384.
[19] Zhang, Y., Sundararajan, S. (2005). The effect of autocorrelation length on the real area of contact and friction behavior of rough surfaces. *Journal of Applied Physics*, 97(10).
[20] Zhang, Y., Sundararajan, S. (2006). Generating random surfaces with desired autocorrelation length. *Applied Physics Letters*, 88(14).
[21] Bažant, Z. P., Pang, S.-D. (2007). Activation energy based extreme value statistics and size effect in brittle and quasibrittle fracture. *Journal of the Mechanics and Physics of Solids*, 55(1):91–131.
[22] Moon, K. H., Falchetto, A. C. (2015). Microstructural investigation of hot mix asphalt (HMA) mixtures using digital image processing (DIP). *KSCE Journal of Civil Engineering*, 19:1727–1737.
[23] Cailletaud, G., Jeulin, D., Rolland, P. (1994). Size effect on elastic properties of random composites. *Engineering Computations*, 11(2):99–110.
[24] Matheron, G. (1991). *Random sets and integral geometry*. John Wiley & Sons, Ltd.
[25] EN 197-1:2011. *Cement Part 1: Composition, specifications and conformity criteria for common cements*.
[26] EN 12620:2013. *Aggregates for concrete*.
[27] EN 933-1:2012. *Tests for geometrical properties of aggregates - Part 1: Determination of particle size distribution - Sieving method*.
[28] EN 206-1:2000. *Concrete - Part 1: Specification, performance, production and conformity*.